FATIGUE CRACK PROPAGATION AND CRACK CLOSURE IN GREY AND AUSTEMPERED DUCTILE CAST IRONS

LI WENFONG* and M N JAMES†

* *School of Process and Materials Engineering, University of the Witwatersrand, WITS 2050, Johannesburg, South Africa*
† *School of Manufacturing, Materials and Mechanical Engineering University of Plymouth, Drake Circus, Plymouth Devon PL4 8AA, England*

ABSTRACT

Fatigue crack propagation behaviour in regions I and II, together with crack closure data have been obtained and compared for an austempered ductile cast iron (ADI) and a grey cast iron (GI) at load ratios (R) of 0.1 to 0.5. A load-shedding technique was applied to SENB4 specimens and crack closure was monitored via a back-face strain gauge. A 'knee' was not observed in the growth rate curves for the GI, but was observed in the case of the ADI. The driving force, as measured by ΔK or ΔK_{eff}, required to produce equivalent growth rates in the two grades of cast iron, was higher in the case of the GI at growth rates $< 10^{-5}$ mm/cycle, but this reverses at higher growth rates because of the greater slope of the growth rate curves observed with the GI. This appears to be a result of the rougher fracture surface found with the GI, coupled with its higher sensitivity to K_{max}-induced brittle fracture. Crack propagation in this material occurs by forming a number of graphite flake-induced cracks ahead of the existing crack tip, and coalescence of these leads to crack branching, an extremely rough fracture surface, and a meandering crack path.

KEYWORDS

Fatigue crack growth, threshold, crack closure, austempered ductile cast irons, grey cast irons.

INTRODUCTION

Austempered ductile irons are a relatively new class of cast irons which have excellent combinations of strength, ductility and wear resistance [1, 2]. Grey cast irons are still used widely because of their excellent corrosion resistance and good wear resistance, coupled with low cost. Fatigue data for such materials is still somewhat limited, particularly crack growth rate curves. Equally, the observed behaviour can be quite variable, as reported in the literature [3]. It is therefore necessary to investigate fatigue crack growth and crack closure in such materials; particularly the influence of environment, as cast irons often find application in harsh conditions, e.g. in mining. This study considered the effect of air and mine water environments on fatigue crack growth in ADI and GI specimens, although only the results of the air experiments are reported here.

EXPERIMENTAL PROCEDURES

Material Characterisation

ADI specimens were cut from specially cast blocks supplied by SALCAST, while GI specimens were cut from the casing of a failed blower. Final specimen dimensions were 10x30x200 mm, with the samples being cut approximately to size and heat treated prior to final machining. The chemical composition of the two cast irons are shown in Table 1.

Table 1 Chemical compositions of ADI and GI (wt%)

	C	Si	Mn	S	P	Ni	Cr	Cu	Mo	Mg
ADI	3.53	2.45	0.21	0.003	0.033	0.12	0.05	0.61	0.005	0.054
GI	3.38	3.00	0.65	0.13	0.58	0.04	0.07	0.12	0.01	0.005

Ductile cast iron specimens were austenitised at 950°C for 2 hours, quenched in a salt bath at 350°C for ½ hour, and then cooled in air to room temperature. The transfer of specimens from the furnace to the salt bath was very rapid, to ensure that the austenite formed at high temperature would not transform to pearlite. Grey cast iron specimens were given a stress relief heat treatment at 550°C for 2 hours, followed by cooling in air to room temperature. SEM micrographs of their structures are given in Fig. 1, both before and after etching in 2% Nital.

Mechanical properties were measured for the two irons (in the case of the ADI both before and after heat treatment) and the data are given in Table 2. Results are given as average values from four tests, but it is worth noting that the GI showed significant variation in strength (as much as about 50% in eight tests with specimens from different regions), due to local variations in graphite flake size.

Table 2 Typical mechanical properties of the two cast irons

	Vickers Hardness	Charpy Impact Energy J	Yield Strength MPa	Tensile Strength MPa
As-received Ductile Iron	267	4	455	846
ADI	337	10.5	770	1026
GI	207	2.5	148	207

Experimental Conditions

Testing was performed using a 50 kN ESH servo-hydraulic testing machine with computer control and automatic data logging of closure values. Four-point SENB specimens were used and data were obtained for stress ratios between 0.1 and 0.5. Crack length monitoring was via optical travelling microscope and cellulose acetate replicas. Tests were periodically interrupted and the specimen held at mean load during crack length measurement. Test frequency was 40 Hz during crack growth and 1 Hz during closure measurements. Crack closure was monitored via a back-face strain gauge and a strain amplification card in the computer. During closure measurement, the minimum load in the cycle was taken as close as possible to zero.

A load shedding procedure was adopted to determine the crack growth rate curve. Initial ΔK values were 20 MPa$\sqrt{m}$ for the ADI and 10 MPa$\sqrt{m}$ for the GI. Cracks were developed and grown around 2 mm beyond the notch root, prior to commencement of the threshold test. Test procedure generally followed the requirements of ASTM E647-86a. Stress intensity ranges were decreased until growth rates ~ 10^{-6} - 10^{-7} mm/cycle were obtained. An increasing ΔK was then applied to detect whether data were influenced by any artifacts of the load shedding procedure. No difference between load decreasing and load increasing data were observed.

RESULTS AND DISCUSSION

Growth rate data are presented in Fig. 2, plotted against the range of applied stress intensity factor, ΔK, and against the effective value, ΔK_{eff}, after factoring out closure. The minimum growth rates obtained in testing represent a situation of no detectable growth in several million cycles. It can be seen that cracks in the GI arrested at relatively high growth rates (~ 10^{-6} mm/cycle), while the ADI material exhibits more usual behaviour with growth rates extending down to around 10^{-7} mm/cycle. The reason for this is believed to be the cracking behaviour shown by the GI grade, in which crack extension involves branching and development of parallel cracks on displaced planes near the crack tip (Fig. 3). In the case of the ADI, crack growth is macroscopically fairly planar (Fig. 3).

There are two points of significant interest in the growth rate data:

- Firstly, the existence of a 'knee' in the growth rate curves for the ADI material, which is not apparent in the GI grade.
- Secondly, the fact that use of ΔK_{eff} affords some rationalisation of growth rate data for both grades in the threshold regime, while little reduction in growth rate variability occurs at higher ΔK values.

A 'knee' in the crack growth rate curve has been shown to occur when the cyclic crack tip plastic zone size becomes of same the order as the dominant microstructural dimension. Crack growth then becomes confined more to crystallographic slip directions and the change in mechanism leads to increased surface roughness, whilst the crack tip opening displacement is reducing, and this leads to a change in slope for growth rate. The ADI contains spheroidised graphite nodules around 80 μm in diameter, and has a fine scale bainitic structure. Thus the change in cyclic crack tip plastic zone size, from 100 μm at 20 MPa$\sqrt{m}$ to 10 μm at 5 MPa$\sqrt{m}$ has a pronounced effect on growth mechanism. The 'knee' in the growth rate curves (≈ 10 MPa$\sqrt{m}$) corresponds to a plastic zone size of around 30 μm, which is around the order of the bainite packet size.

However, in the GI grade the crack tip cyclic plastic zone size, which changes only from 90 μm at 11 MPa$\sqrt{m}$ to 50 μm at 8 MPa$\sqrt{m}$, is a secondary influence on crack mechanism compared with the scale of the graphite flakes. Hence crack growth in the GI reflects microstructural features (graphite flake size and distribution) over the whole range of growth rates considered.

The observation that growth rate variability is reduced in ADI through the use of ΔK_{eff}, but not

in GI is clarified through consideration of the closure data, presented in Fig. 4 as the ratio P_{op}/P_{max} against ΔK. For the ADI grade, it appears that the closure data for all the stress ratios fits onto a single curve, at least within the bounds of 'normal' variability. Closure appears to increase from a more-or-less constant value of around 0.15 at ΔK values in the linear growth rate regime, to a value of around 0.40 at the threshold for crack growth. The increase in closure value correlates well with the 'knee' in the growth rate curve, i.e. $\Delta K \approx 10$ MPa$\sqrt{m}$. A reasonable interpretation of this data is that plasticity-induced closure has a fairly stable value of around 0.15 in the linear growth rate regime. This implies that plasticity-induced closure scales with plastic zone size. Other closure mechanisms, such as surface roughness-induced and oxide-induced closure begin to play a dominant role in the threshold regime and closure values increase. Stress ratio does not appear to have a strong influence on measured closure values. Note that the closure ratio is defined in the same way as the stress ratio ($R = K_{min}/K_{max}$) and thus closure only has an influence on the applied fatigue cycle when $P_{op}/P_{max} > R$, i.e. throughout the crack growth rate range for $R = 0.1$, for $\Delta K <$ 8-10 MPa$\sqrt{m}$ when $R = 0.2$ or 0.3, and around the threshold when R = 0.4.

This explains the effect of ΔK_{eff} on the growth rate curve for ADI; in the threshold regime, a useful rationalisation of data is effected, but in the linear growth rate regime there is little closure influence and data are largely unchanged. It is likely that K_{max} is influencing growth rates in this regime, as fracture processes in the cast iron would be sensitive to this parameter. As $\Delta K = K_{max}(1 - R)$ and considering a ΔK value of 20 MPa$\sqrt{m}$, K_{max} varies from about 22 MPa$\sqrt{m}$ at $R = 0.1$ to 40 MPa$\sqrt{m}$ at $R = 0.5$. As can be seen in the data for $R = 0.5$, growth rates are starting to increase exponentially at $\Delta K =$ 20 MP$\sqrt{m}$ as $K_{max} \rightarrow K_c$.

In the GI material, however, closure values are reasonably constant irrespective of ΔK (except for $R = 0.1$ where closure increases from about 0.1 at $\Delta K = 11$ MPa$\sqrt{m}$ to around 0.2 at the threshold), but are quite markedly influenced by stress ratio. Closure occupies a relatively small percentage of the applied fatigue cycle, however, and although a small rationalisation of growth rate data occurs near the threshold at $R = 0.1$ through use of ΔK_{eff}, overall the curves are little changed. The reason for the increase in closure as stress ratio increases is not clear, but it can reasonably be surmised that it is related to an effect of K_{max} on surface roughness. At a ΔK value of 10 MPa$\sqrt{m}$, K_{max} changes from 11.1 MPa$\sqrt{m}$ at $R = 0.1$ to 20 MPa$\sqrt{m}$ at $R = 0.5$. The GI grade is far more brittle than the ADI, and this change in K_{max} is likely to enhance fracture at graphite flakes and lead to an increase in out-of-plane deviations in the crack path, which would tend to increase any surface-roughness induced component of closure (which in this material is probably at least as important in this growth rate regime as plasticity-induced closure). Figs. 5 and 6 show fractographs for the two irons, which are representative of growth in the threshold regime and at the upper end of the ΔK values considered.

The net effect of these interactions on growth rate in the two irons, is that GI displays a better resistance to crack growth when $da/dN < 10^{-5}$ mm/cycle than ADI but, due to the greater slope seen in its growth rate curves compared with those for the ADI, a lower resistance at growth rates higher than this value. Crack growth rate tests in a mine water environment are in progress, and it will be interesting to see what effect this has on crack growth behaviour in the two irons.

CONCLUSIONS

1. Crack growth rate data for the GI does not display a 'knee' over the range 10^{-4} mm/cycle to 10^{-6} mm/cycle. In contrast, ADI does show a knee at a growth rate of around 10^{-5}mm/cycle. This behaviour holds at all stress ratios examined ($R = 0.1$ - 0.5).

2. Crack closure data for the ADI is reasonably well fitted by a single curve, irrespective of stress ratio. Closure values increase from around 0.15 at $\Delta K >$ 10 MPa$\sqrt{m}$ to around 0.40 - 0.45 at the threshold.

3. Crack closure data for the GI show a clear effect of the value of stress ratio. At $R = 0.1$, a slight increase in closure ratio (from about 0.1 to 0.2) is observed as ΔK decreases from 11 MPa$\sqrt{m}$ to 9 MPa$\sqrt{m}$. For $R = 0.2$ and 0.3, the closure ratio does not appear to change as ΔK decreases but the ratio P_{op}/P_{max} increases to about 0.25 and 0.32 respectively.

4. Use of ΔK_{eff} affords some rationalisation of growth rate data in the threshold regime for the two irons, but not at higher values of ΔK. Data at the higher values of ΔK are believed to be influenced by K_{max} in the fatigue cycle, which will promote brittle fracture, particularly in the GI grade, as ΔK and R increase.

REFERENCES

1. K G Budinski (1994), *Engineering Materials - Properties & Selection*, 4th edition, 524-525, 515-516.
2. N A Waterman (1991), Materials engineering for deep mining, *Applications Materials & Design*, Vol.12 No.1, 15-19.
3. L Haenny and G Zambelli (1985), Crack growth resistance of grey cast iron, *Engineering Fracture Mechanics*, Vol. 21 No. 3, 529-535.

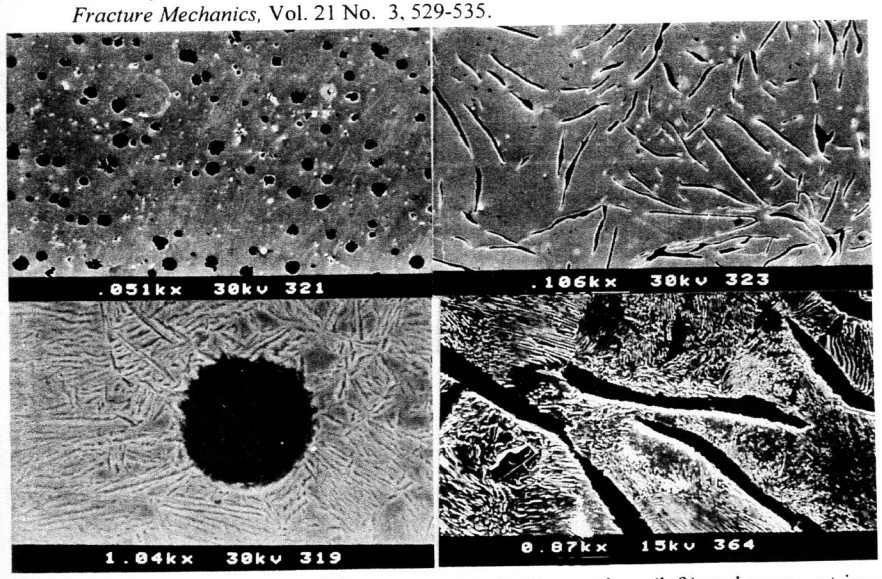

Fig.1 Typical microstructures of the austempered ductile cast iron (left) and grey cast iron (right). *a) b)* (top) un-etched specimens; *c) d)* (bottom) etched in 2% Nital.

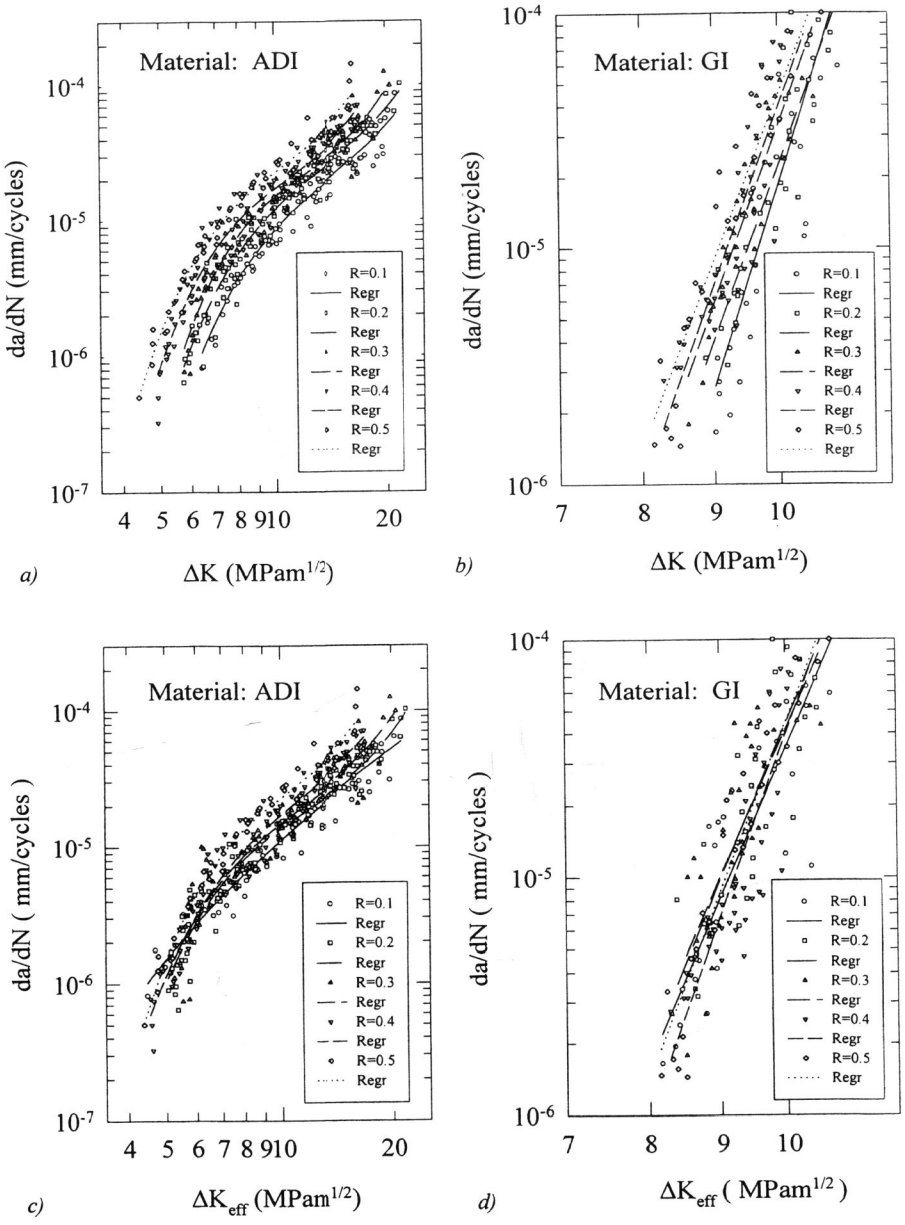

Fig.2. Relationships between crack growth rate and :
a) b) applied stress intensity factor range ΔK; *c) d)* ΔK_{eff}

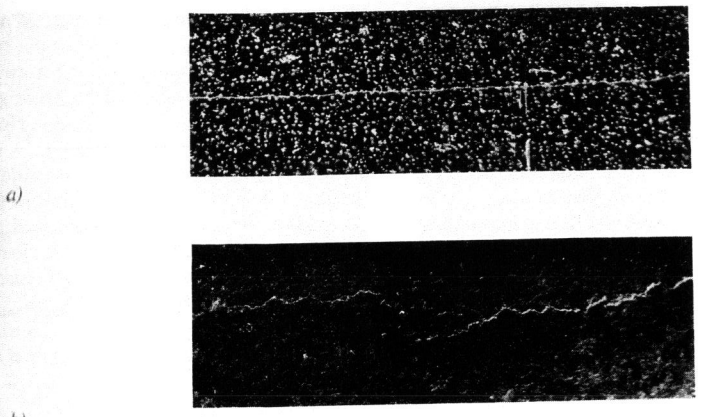

Fig.3 Illustration of the macroscopic crack path in
a) ADI (Magnification 10X) *b)* GI (Magnification 10X)

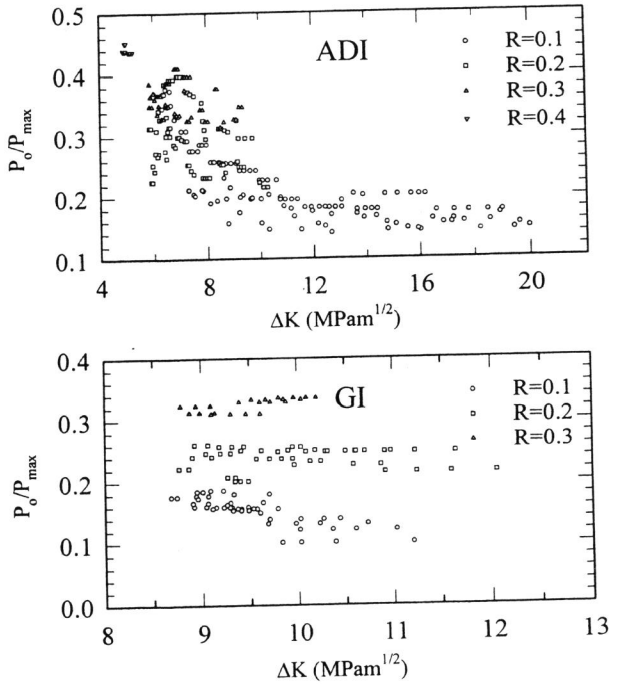

Fig. 4 Closure values, quantified as P_o/P_{max} , plotted against ΔK for *a)* ADI *b)* GI.

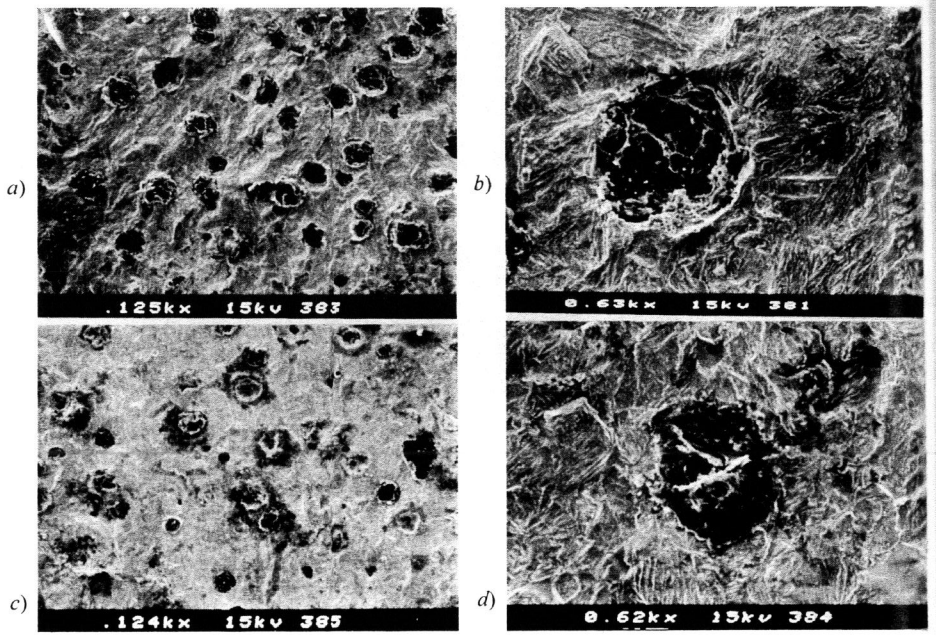

Fig. 5 Typical fractographs for the ADI: *a*) *b*) high ΔK values; *c*) *d*) threshold ΔK values.

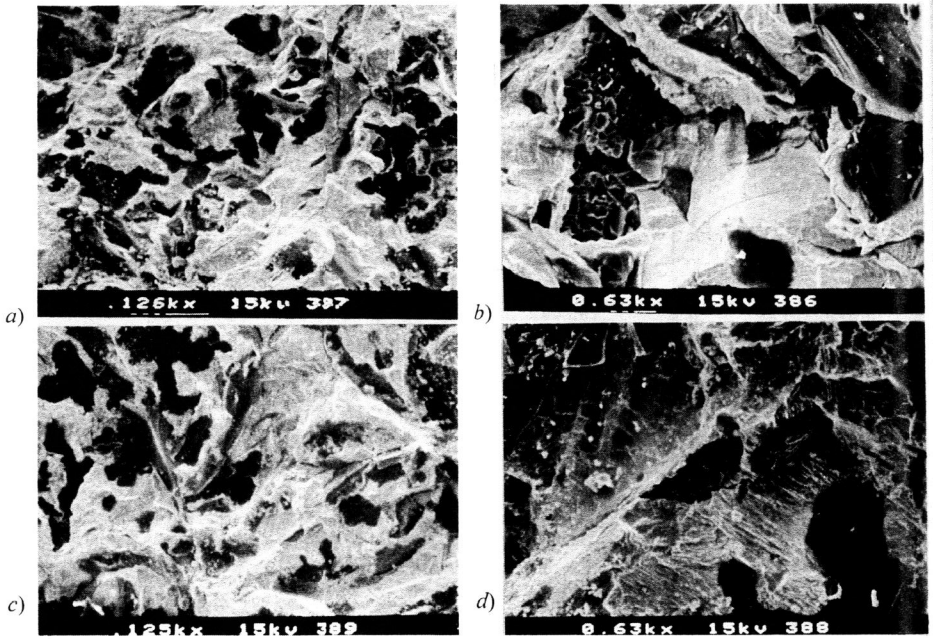

Fig. 6 Typical fractographs for the GI: *a*) *b*) high ΔK values; *c*) *d*) threshold ΔK values.